DEVELOPMENT AND CHARACTERIZATION OF TUBULAR CERAMIC MEMBRANES PRODUCED FROM AN ALUMINA RESIDUE

Guimarães I; Lira H; Guimarães E; Sidinei K. da Silva SK

Universidade Federal de Campina Grande, UFCG, Paraíba, Brazil.

Abstract

Industrial wastes reuse becomes attractive to raw materials economy and to avoid environmental problems. This research objective was to develop and characterize tubular ceramic membranes using in their composition a residue generated during alumina calcination process, known as electrostatic precipitator dust or ESP dust (an alumina residue). Initially, was performed the characterization of the alumina dust. As verified by XDE, the residue showed a high content of Al_2O_3 (about 96%) in its chemical composition. Gibbsite and α-alumina phases were identified by XRD. At SEM images, could be observed agglomerates with asymmetric shapes. A laser particle analyzer showed particles with medium diameter of 15.68μm. In this study, tubular membranes composed by alumina residue and bentonite clay were produced by extrusion, allowing its use on tangential flow, and sintered at 1000°C. Then, they were characterized by SEM, mercury intrusion porosimetry and flow measurements with distilled water. The pore diameter average indicated that the obtained membranes can be applied in microfiltration process.

1. Introduction

A membrane can be defined as a barrier which keeps apart two phases and which restricts, in whole or in part, the transport of one or more chemical species present in phases (Habert et al., 2006).

Synthetic membranes have emerged as an effort to reproduce natural membranes and are manufactured from two distinct materials classes: organic materials, mostly polymers, and inorganic, such as ceramic, carbon, metal and glass (Habert et al., 2006).

Ceramic membranes have been increasingly used in several industries, because they can offer some advantages over polymer membranes, especially in regard to chemical and biological stability and high temperatures and pressures resistance. Another important advantage is that the ceramic membranes have about to traditional separation methods (distillation, centrifugation, etc.), like low power consumption, long life, little space occupying and ease to cleaning (Bhave, 1991 and Boddeker, 1995).

However, these membranes have a high cost of manufacture as disadvantage. Consequently, a large number of studies have focused on developing new ceramic membranes types and their application processes in last years. Various materials have been used in these membranes manufacture, among which are highlighted alumina, silica, zirconia and titania (Burggraaf & Cot, 1996).

Meanwhile, in Brazil, many researchers have intensified their studies about waste recycling to use as a raw materials alternative for various industrial purposes. Some wastes properties allows the incorporation of these residues into ceramic masses to several products manufacture, partial or total replacement of conventional raw materials commonly used in these masses formulation (Brasileiro, 2005).

The residue generated during alumina calcination process is a product with small particle size, commonly called electrostatic precipitator dust or ESP dust. This waste is a heterogeneous product composed by α-alumina, different transition aluminas and hydroxides which did not completed their calcination process (Sancho et al, 2009 and Ayala et al, 2010).

This residue disposal creates several problems, as this dust can be about 5-10% by the total amount of alumina recovered from calciner (Patent, 1986). It is stored indefinitely in waste lakes, red mud pools, so appears the necessity to reuse it (Sancho et al, 2009).

Therefore, ceramic membranes preparation, whose main component is an alumina residue, it becomes very attractive as a better raw materials economy (sustainability) and as also to prevent environmental problems.

2. Experimental

2.1 Residue Characterization

Initially, was done the characterization of an alumina electrostatic precipitator residue sample. The material had a grayish color, which may indicate soot presence resulting of BPF oil poor combustion used on alumina calcination step.

The sample chemical composition analysis, checked using X-ray fluorescence spectroscopy by dispersive energy (XDE) showed a high content of alumina, around 96%, and at a thermal analyzer, was found 14.9% of loss on ignition (LOI) up to 1000°C (Table 1).

Table 1 - Dried alumina residue chemical analysis (wt %).

Al_2O_3	SiO_2	SO_3	Na_2O	CaO	K_2O	CuO	LOI
95.8	1.7	1.6	0.8	0.05	0.03	0.02	14.9

By X-ray diffraction (XRD) was observed aluminum hydroxide or gibbsite phase presence (PDF 74-1775 standard file) and α-alumina (PDF 81-1667 standard file); the gibbsite phase ($Al(OH)_3$) was predominant in alumina residue (Figure 1). Results interpretation was made by comparison with Powder Diffraction File 02 software standards (PDF - 02) of International Center for Diffraction Data (ICDD, 2003).

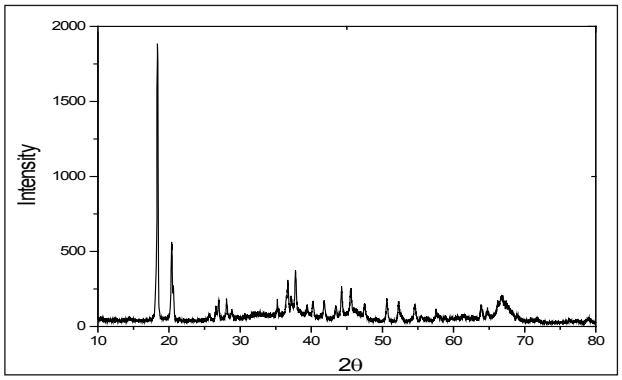

Figure 1 - Alumina residue X-ray diffractogram, where G: Gibbsite and α, α-alumina.

The sample was also analyzed in a laser diffraction granulometry, where was determined an average particle diameter equal to 15.68 μm (Table 2), and at a scanning electron microscope (SEM) as well. At sample micrographs, shown in Figure 2, can be observed the agglomerates and overlaps present, the size and particles distribution and also their morphology. Micrographs shows agglomerates with asymmetric shapes and large particles size distribution, which is in accordance with results obtained in laser diffraction particle size technique, as can be seen in Table 2.

Table 2 - Alumina residue particle size distribution (μm).

Diameter at 10% (D_{10})	Diameter at 50% (D_{50})	Diameter at 90% (D_{90})	Average Diameter (D_A)
1.34	13.53	32.89	15.68

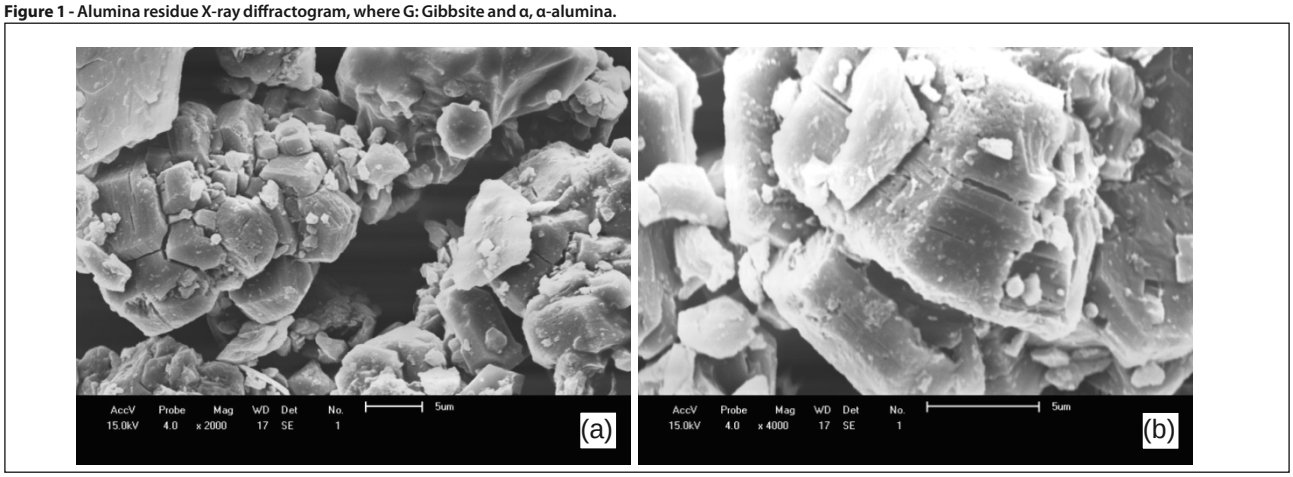

Figure 2 - Alumina residue micrographs: (a) 2000X and (b) 4000X.

2.2 Ceramic Mass

After electrostatic precipitator alumina residue characterizing step, was developed a formulation to produce tubular ceramic membranes, a mixture composed by the alumina residue (70wt%) and bentonite clay (30wt%). The clay gives plasticity to the ceramic mass and enables its processing by extrusion.

Residue and clay were manually mixed, after this was added liquid additives and water, and then the components were homogenized until get a uniform plastic mass with 28% moisture content. This mass was packed in a sealed plastic bag to retain the moisture and after four days rest, was shaped by extrusion (Figure 3).

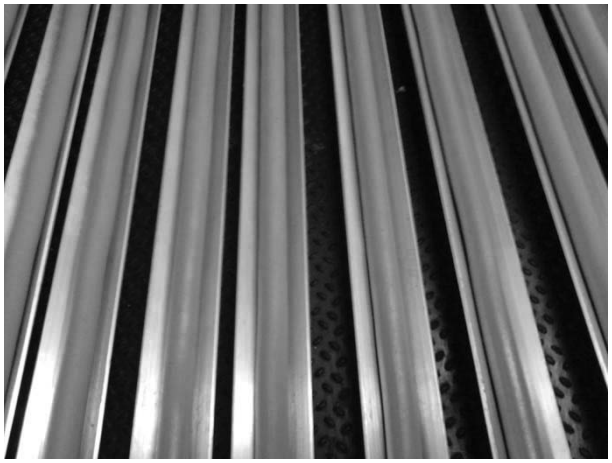

Figure 3 - Tubular membranes obtained by ceramic mass.

After extrusion step, the membranes were dried slowly in humid atmosphere at room temperature during 14 days, then were dried at 60°C for 24h and then at 100°C for 24h. After drying, the tubular membranes were cut to 8 cm long and sintered in an electric furnace, where were submitted to a heating curve up to 1000°C (maximum temperature), shown in Table 3 below.

Table 3 - Membranes sintering heating curve.

Temperature	Heating rate	Baseline
Room temperature - 400°C	3°C/min	-
400°C - 700°C	2°C/min	-
700°C - 1000°C	4°C/min	60 minutes

Membranes sintering was done based on ceramic mass thermal analysis curves (Figure 4), where can be analyzed the thermogravimetric analysis (TGA) and differential thermal analysis (DTA) curves.

In Figure 4 it may be noted in TGA curve a 2.3% of mass loss up to 200°C, due to adsorbed water loss. Between 200°C and 400°C there is a mass loss of 7.7% due to the loss of gibbsite hydroxyl groups. Between 400°C and 700°C there is 5.6% of mass loss, as a possible result of bentonite clay hydroxyl groups loss and organic matter loss. From 700°C until the end of experiment still occurs 1.5% of mass loss. Total mass loss was 17.1%.

Also in Figure 4, it can be seen in DTA curve an endothermic peak at 131.8°C, characteristic of adsorbed water presence, and two others endothermic peaks, one at 249.3°C and another intense at 330.1°C, associated with gibbsite hydroxyl groups presence. It can be observed even an endothermic peak at 563.9°C, followed by an exothermic peak at 621.3°C, which may be correlated with bentonite clay hydroxyl groups presence and organic matter, respectively. A small exothermic peak at 923.1°C was observed as well, related to material phase transformations.

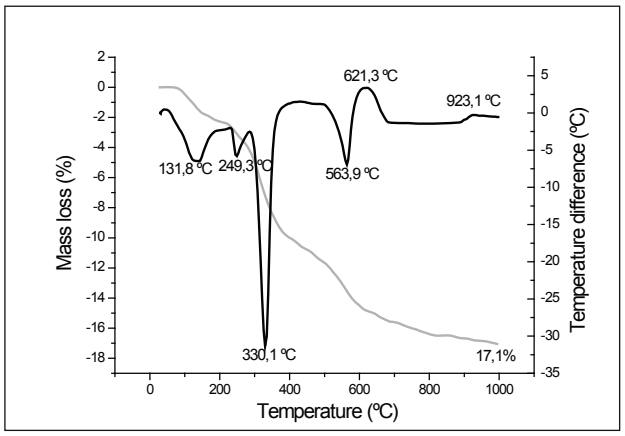

Figure 4 - Ceramic mass TGA/DTA curves obtained with a 12.5°C/min heating ratio.

2.2.1 Ceramic mass characterization

The ceramic mass was characterized before and after being sintered.

2.2.1.1 Before sintering

The ceramic mass was analyzed by XDE, where were checked high contents of alumina (Al_2O_3) e sílica (SiO_2) on chemical composition, around 70% of Al_2O_3 and 24% of SiO_2. At a thermal analyzer, was found 16.35% of loss on ignition (LOI) by 1000°C (Table 4).

Table 4 - Dried ceramic mass chemical analysis (wt %).

Al_2O_3	SiO_2	MgO	SO_3	Fe_2O_3	CaO	TiO_2	K_2O	BaO	CuO	ZnO	LOI
70.091	24.228	2.286	1.077	1.064	0.618	0.324	0.227	0.075	0.007	0.004	16.35

The sample was also evaluated by laser diffraction particle size and the average particle diameter was equal to 11.33 µm (Table 5), lower than that was found previously for pure alumina residue (D_A = 15.68 µm), principal ceramic mass component (70 wt%).

Table 5 - Ceramic mass particle size distribution (µm).

Diameter at 10%	Diameter at 50%	Diameter at 90%	Average Diameter
1.38	9.00	24.30	11.33

Using a soil sample metal mixing bowl, were obtained Atterberg limits, which determine the ceramic mass plasticity and are important to verify the possibility of its extrusion (Table 6). Could be observed that the sample shows 21% of plasticity index; being considered highly plastic and ideal for shaping by extrusion method. The high plasticity is attributed to bentonite clay presence.

Table 6 - Ceramic mass Atterberg limits (%).

Liquid Limit (LL)	Plasticity Limit (PL)	Plasticity Index (PI)*
59	38	21

* where: PI = LL – PL

According to Figure 5, the X-ray diffractogram obtained for ceramic mass before be sintered, could be noticed the presence of the phases: aluminum hydroxide or gibbsite (PDF 74-1775 standard file), α-alumina (PDF 81-1667 standard file), kaolinite (PDF 29-1488 standard file) and smectite (Souza Santos, 1989). Kaolinite and smectite phases were originated from bentonite clay used in formulation.

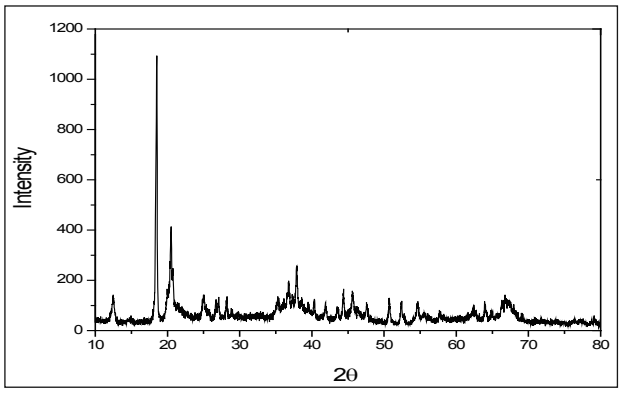

Figure 5 - X-ray diffractogram of ceramic mass before be sintered, where G: Gibbsite, α: α-alumina, K: Kaolinite e S: Smectite.

2.2.1.2. After sintering

In Figure 6, from X-ray diffractogram obtained for ceramic mass after be sintered, was identified the presence of α-alumina (PDF 81-1667 standard file) and mullite (PDF 88-2049 standard file) phases. Mullite phase probably is present in its primary form, as small crystals agglomerates, which usually begin to form at temperatures around 1000°C, the sintering temperature used.

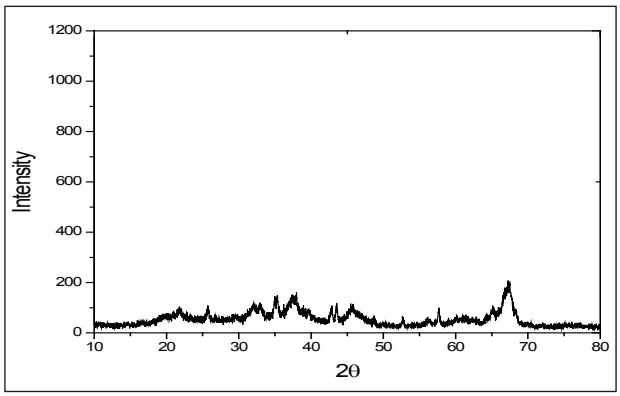

Figure 6 - X-ray diffractogram obtained for ceramic mass after be sintered, where α: α-alumina e M: Mullite.

2.3 Ceramic membranes characterization

The tubular ceramic membranes were characterized by scanning electron microscopy, porosimetry by mercury intrusion and flow measurements with distilled water.

In Figure 7 are present cross sections micrographs of the tubular ceramic membranes sintered at 1000°C. Agglomerates can be detected with asymmetrical shapes on membranes surfaces. It is also observed that the membranes have surfaces with distributed pores and no cracks, characteristics that make them suitable for use in separation processes. From micrographs is not possible to accurately estimate the membrane pores size.

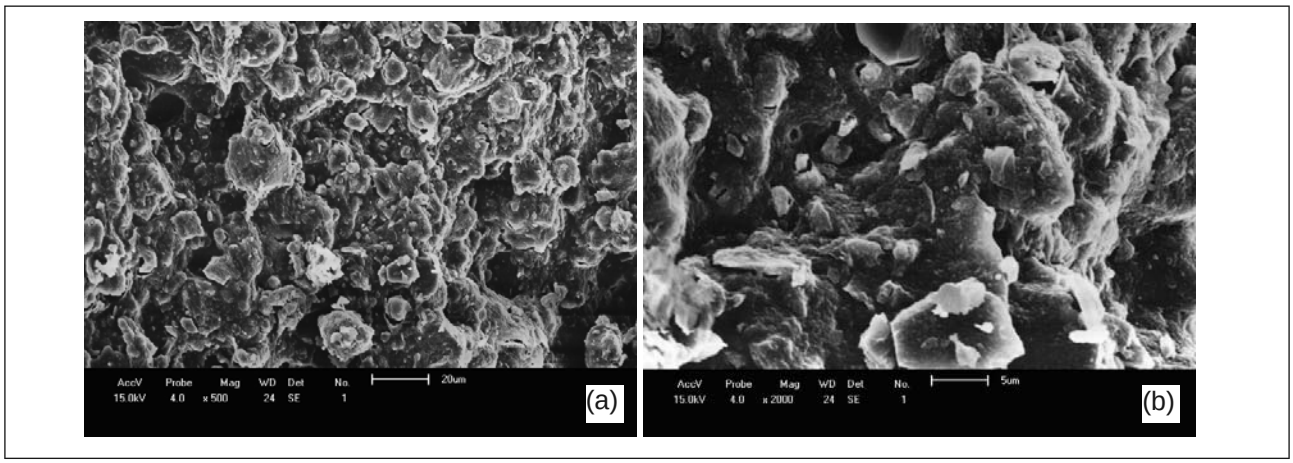

Figure 7 - Cross sections micrographs of the membranes sintered at 1000°C: (a) 500X and (b) 2000X.

Table 7 shows the average pore diameter and porosity of the ceramic membranes sintered at 1000°C and is demonstrate in Figure 8 the variation of ceramic membranes pores diameter based on mercury accumulated intrusion volume.

From Table 7 data, it appears that the membranes produced have 33.96% of porosity and 0.92 µm of average pore diameter, within the range of microfiltration, which comprises membranes with pores between 0.1 to 10 µm. It can be seen in Figure 8 a narrow pore size distribution and, consequently, the obtained membranes probably have high selectivity.

Table 7 - Average pore diameter and porosity of ceramic membranes sintered at 1000°C.

Average pore diameter	Porosity
0.92 µm	33.96%

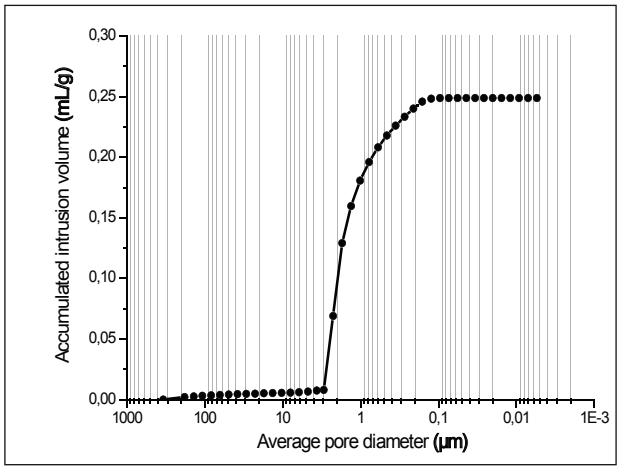

Figure 8 - Average pore diameter variation based on mercury accumulated intrusion volume in membranes.

Results of distilled water permeated by tangential flow through membranes, at 1.0 kgf/cm^2 of pressure, are exposed in Figure 9. Initially, the permeated flux shown high values. Among the membranes examined, the highest permeated flux was observing for sample 3 (777.13 L/h.m^2) at the first minute of system operation. Then, permeated flux was decreasing over time, which may be correlated to membranes hydration. The membranes have α-alumina and mullite in composition and these phases can show, even after being sintered at 1000°C, a large ability to absorb water on its surface, leading to a decrease in pore size and consequently a decrease in permeated flux. After the membranes hydration period, at about 2h, the flow remained constant. At this point, the flow has stabilized below 10% of initial value, at 53.53 L/h.m^2 for sample 3.

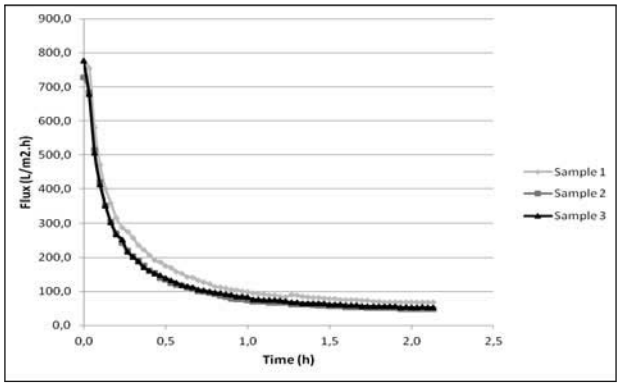

Figure 9 - Permeated flux of distilled water through ceramic membranes sintered at 1000°C.

3. Conclusions

From the development and characterization of ceramic tubular membranes produced from an alumina electrostatic precipitator residue could be concluded that:

- The residue chemical composition showed a high content of alumina, around 96%, and was found a loss on ignition of 14.9% up to 1000°C;
- The present phases in residue were: gibbsite and α-alumina; the gibbsite phase was predominant in sample;
- The sample showed an average particle diameter equal to 15.68 µm;
- At alumina residue was observed agglomerates with asymmetric shapes, overlaps and a large particles size distribution;
- In the ceramic mass was found a total mass loss of 17.1% and a loss on ignition of 16.35% by 1000°C;
- The ceramic mass chemical composition showed high contents of alumina and silica, about 70% of Al2O3 and 24% of SiO2;
- The ceramic mass showed an average particle diameter equal to 11.33 µm and was considered highly plastic (PI=21%), ideal for shaping by extrusion method;
- The present phases in ceramic mass before sintering were: α-alumina, gibbsite, kaolinite and smectite, and after sintering: α-alumina and mullite;
- Agglomerates can be detected with asymmetrical shapes on membranes surfaces. It is also observed that the membranes have surfaces with distributed pores and no cracks, characteristics that make them suitable for use in separation processes. From micrographs is not possible to accurately estimate the membrane pores size;
- The membranes produced had 33.96% of porosity and 0.92 µm of average pore diameter, within the range of microfiltration;
- Initially, the permeated flux showed high values and then it was decreasing over time, which may be correlated to membranes hydration. The membranes have α-alumina and mullite in composition and these phases can show, even after being sintered at 1000°C, a large ability to absorb water on its surface, leading to a decrease in pore size and consequently a decrease in permeated flux. Among the membranes examined, the highest permeated flux was observing for sample 3 (777.13 L/h.m2) and after membranes hydration period, the flow remained constant. At this point, the flow has stabilized at 53.53 L/h.m2 for sample 3;
- The tubular ceramic membranes produced from an alumina electrostatic precipitator residue can lead to a technological revolution, because it adds economic value to this material, which is produced in large quantities around the world and is still without much application.

4. Thanks

Many thanks to Petroleum, Natural Gas and Biofuels National Agency (ANP) for all support provided to carry out this research.

References

AYALA, J.; FERNANDEZ, B.; SANCHO, J. P.; GARCIA, P. **Synthesis of Three Commercial Products from Bayer Electrofilter Powders.** Journal of Hazardous Materials 178, p. 758-765, 2010.

BHAVE, R. R. **Inorganic Membranes Synthesis. Characteristics and Applications.** 1ª Ed., New York: Van Nostrand Reinhold, 1991. 19p.

BODDEKER, K. W. **Commentary: Tracing Membrane Science.** Journal of Membrane Science 100, p. 65-68, 1995.

BRASILEIRO, M. I. **Obtenção de Mulita a partir de Resíduo de Caulim**. Dissertação de Mestrado, Engenharia Química, UFCG, Campina Grande, PB, 2005.

BURGGRAAF, A. J.; COT, L. **Fundamentals of Inorganic Membranes Science and Technology**. 1ª Ed., Amsterdam: Elsevier, 1996. 21p.

HABERT, A. C.; BORGES, C. P.; NOBREGA, R. **Processos de Separação por Membranas**. Série: Escola Piloto em Engenharia Química, COPPE/UFRJ. Rio de Janeiro: E-papers, 2006.

ICDD - International Center for Diffraction Data, **Powder Diffraction File 02 (PDF - 02),** 2003.

Patent nº 4568527, February 4, 1986. **Utilization of Partially Calcined Alumina as Precipitation Aid in the Bayer Process**. Expected Date: November 6, 2004. Available at: <http://www.patentstorm.us/patents/4568527/description.html>. Accessed: February 12, 2011.

SANCHO, J.; FERNÁNDEZ, B.; AYALA, J.; GARCÍA, P.; VERDEJA, L. F. **The Recycling of Bayer Electrofilter Fines for Diverse Applications.** 1st Spanish National Conference on Advances in Materials Recycling and Eco-Energy, S04-9, Madrid, 12-13 November 2009.

SOUZA SANTOS, P. **Ciência e Tecnologia de Argilas**. 2ª Ed. revisada e ampliada. v. 1, São Paulo: Edgard Blucher Ltda, Escola Politécnica da USP, 1989.